ISSN 1392–1320 MATERIALS SCIENCE (MEDŽIAGOTYRA). Vol. 31, No. 1. 2025

Study on Phase Evolution of Calcium Silicate Hydrate (C-S-H) During Solidification of Cr(VI) under Hydrothermal Conditions

Zhiguang ZHAO, Xiaoling QU *, Zhanming LI, Changan TIAN, Zaibo LI

School of Chemical and Civil Engineering, Shaoguan University, Shaoguan 512005, China

http://doi.org/10.5755/j02.ms.38311

Received 6 August 2024; accepted 26 September 2024

In this paper, calcium silicate hydrate (C-S-H) was synthesized by hydrothermal method using CaO and quartz sand as raw materials. The solidification effect of Cr(VI) in C-S-H was studied using XRD, FTIR, and SEM. The leaching amount of Cr(VI) after solidification was determined by anatomic absorption spectrometer to analyze and calculate the solidification rate of Cr(VI). Results show that appropriately increasing the reaction temperature and prolonging the reaction time can help improve the crystallinity of C-S-H. A small Cr(VI) dosage of Cr/Si < 0.05 is beneficial for the crystallization of C-S-H, but when Cr/Si > 1.0, Cr(VI) ions inhibit the formation of C-S-H. When Cr/Si <0.15, the solidification efficiency of C-S-H on Cr(VI) decreases with increasing Cr(VI) content; The C-S-H with Ca/Si = 1 has the best solidification efficiency for Cr(VI).

Keywords: calcium silicate hydrate (C-S-H), hydrothermal condition, phase changes, solidification, Cr(VI).

1. INTRODUCTION

Currently, the amount of solid waste is also increasing, according to statistics, nearly 3 billion tons of industrial solid waste are generated in China every year [1]. Solid waste contains a large amount of heavy metal elements, such as, chromium (Cr), cadmium (Cd), lead (Pb), copper (Cu), zinc (Zn), nickel (Ni), Neptunium (Np), arsenic (As), etc., which have certain toxicity and pose a threat to human health and the environment. Heavy metals can strongly interact with proteins and enzymes in the human body, causing them to lose their activity and potentially accumulate in certain organs, leading to chronic poisoning. Taking chromium as an example, Cr(VI) can invade the human body through the digestive tract, respiratory tract, skin, and mucous membranes, causing mild damage to the skin, severe damage to the respiratory and digestive tracts, and even causing cancer.

Therefore, how to achieve the "harmlessness", "reduction", and "resource utilization" of solid waste is a major issue that China urgently needs to solve [2]. The main methods for treating solid waste include landfill, incineration, and solidification/stabilization technology. In comparison, solidification/stabilization technology is a promising approach.

Solidification/stabilization technology is a treatment technique that utilizes solidification/stabilizers to form essentially insoluble substances in hazardous waste or encapsulate them in inert waste forms. The most commonly used method is to use cement, plastic, water glass, asphalt, etc. as setting agents and mix them with hazardous waste for solidification [3–9]. Nowadays, the solidification method has become one of the main methods for treating toxic substances in waste, and cement-based materials are the most widely and frequently used materials in the solidification of heavy metals in waste in developed countries such as Europe and America in recent years. The high pH value of cement-based materials can cause almost all heavy metals to form insoluble hydroxides or carbonates and be solidified in the solidified body [10–13]. Calcium silicate hydrate (C-S-H) is the main product of cement hydration, with a content of up to 70 %, and is the main solidified form. C-S-H is usually the main carrier of foreign metal elements, and it has a strong ability to accommodate heavy metals.

Recently, the solidification/absorption of various heavy metal ions, such as bivalent ions (Zn (II), Pb (II), etc.) [14], and trivalent and tetravalent metal ions (Cr (III), Np (IV), etc.) [15] by C-S-H has been investigated. C-S-H replaced by ions becomes a component of cement and can maintain stability. This approach has been studied for decades, but there are still some challenges that need to be overcome in terms of the correlation between heavy metal ions, especially Cr (VI), and the C-S-H structure, as well as the resulting compounds.

As is well known, the solidification of heavy metal ions in the C-S-H structure depends on factors such as the characteristics of metal ions and the hydrothermal treatments. The C-S-H structure can affect the interaction of heavy metal ions. Compared with crystals, C-S-H gel has a larger specific surface area, resulting in stronger adsorption capacity. For example, its adsorption rates for Cd (II), Zn (II), Pb (II), and Cr (III) exceed 99.96 % [16]. At the same time, these heavy metal ions can affect the recombination and crystallization of C-S-H structures.

In addition, chromium ions can exist in the form of $CaCrO_4$ in the C-S-H and cement solidified body [17]. Previous studies have shown that Cr(Ⅵ) does not affect the principle of the hydration process. The hydration rate of cement is significantly accelerated when the Cr(Ⅵ) content is 2 wt.% [18]. Lv et al. found that when the Cr(Ⅵ) content was less than 0.5 wt.%, the content of f-CaO was reduced. When the Cr(Ⅵ) content was between 1.0–3.0 wt.%, it could cause C_3S to transform into C_2S and CaO, greatly

* Corresponding author: X. Qu
E-mail: *msqxl@sgu.edu.cn*

increasing the content of *f*-CaO [19]. Renata and Jan suggested that Cd (II), Zn (II), Pb (II), and Cr (III) can be effectively solidified by C-S-H, while these ions inhibit the formation of C-S-H. The leaching experiments of Cd, Zn, Pb, and Cr confirmed that the fixation efficiency of Zn and Pb is better than that of Cd and Cr [16]. Omotoso et al. found that an increase in Cr(Ⅵ) content led to a decrease in the crystallinity of C-S-H [20].

Under hydrothermal conditions, the crystallinity of C-S-H increases, and the solidification mechanism of heavy metal ions is different. For example, in the CaO-SiO_2-Al_2O_3-H_2O system (0 – 72 hours, 200 °C, Ca/Si = 1.5), Cr (III), Co (II), or Cu (II) can all enter the C-S-H structure and form individual compounds. Therefore, high ion exchange capacity and specific surface energy enable C-S-H to solidify heavy metal ions through symbiosis, adsorption, and chemical displacement at interlayer positions [21] Some solidification mechanisms have also been proposed. Heavy metal ions are solidified on the surface of C-S-H in the form of hydroxide or complex, or exist in the form of precipitation, which inhibits the leaching of heavy metal ions [22].

The use of cement-based materials can solidify a large amount of heavy metal ions, but during service and after deterioration and structural damage, the heavy metal ions present on the surface of cement hardened bodies are easily affected by environmental conditions. Under acid rain erosion and weathering, there is still a possibility of releasing heavy metals into the environment [18]. Therefore, studying the structural changes of C-S-H during the solidification of Cr (VI) is crucial for the safe and efficient treatment of heavy metals. In view of this, the solidification of Cr (VI) and structural changes of C-S-H were investigated in this paper.

2. EXPERIMENTAL

2.1. Materials

Calcium oxide (CaO, calcined at 950 °C for 3 hours) and finely ground quartz sand were used as raw materials for the synthesis of C-S-H. The particle size distributions of CaO and quartz sand are shown in Fig. 1. Potassium dichromate ($K_2Cr_2O_7$) is chemically pure and purchased from National Pharmaceutical Group Chemical Reagent Co., Ltd.

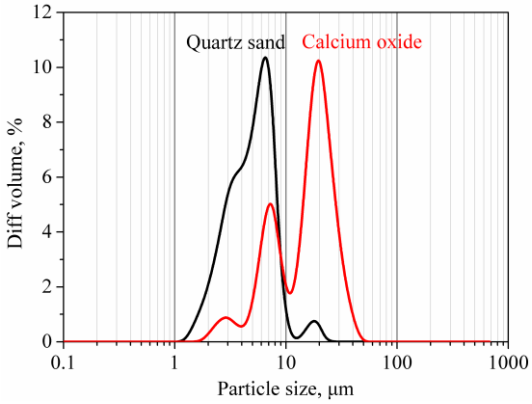

Fig. 1. Particle size distributions of CaO and quartz sand

2.2. Synthesis of C-S-H and solidification of Cr(VI)

Taking the close relationship between the solidification of Cr(VI) by C-S-H and the phase composition of C-S-H, C-S-H with various Ca/Si ratio was synthesized at various reaction temperatures and time, in order to investigate the relationship between the C-S-H and its solidification ability of Cr(VI). The experimental proportions for C-S-H synthesis are shown in Table 1.

Table 1. Proportions for hydrothermal synthesis of C-S-H

No.	CaO, g	Quartz sand, g	Ca/Si	Water, g	Temperature, °C	Time, h
A0	2.8	3	1	30	180	8
B0	2.8	3	1	30	180	4
C0	2.8	3	1	30	180	12
D0	2.8	3	1	30	180	24
E0	2.8	3	1	30	140	8
F0	2.8	3	1	30	220	8
H0	2	4	0.5	30	180	8
K0	3.5	2.5	1.5	30	180	8

Based on the above, Cr(Ⅵ) was added to study the solidification effect of C-S-H on Cr(Ⅵ). The specific experimental design is shown in Table 2.

Table 2. Proportions for solidification of Cr(Ⅵ) by C-S-H

No.	CaO, g	Quartz sand, g	Ca, Si	Water, g	Cr, Si	Tempe-rature, °C	Time, h
A1	2.8	3	1	30	0.05	180	8
A2	2.8	3	1	30	0.10	180	8
A3	2.8	3	1	30	0.15	180	8
B1	2.8	3	1	30	0.10	180	4
C1	2.8	3	1	30	0.10	180	12
D1	2.8	3	1	30	0.10	180	24
E1	2.8	3	1	30	0.10	140	8
F1	2.8	3	1	30	0.10	220	8
H1	2	4	0.5	30	0.05	180	8
H2	2	4	0.5	30	0.10	180	8
H3	2	4	0.5	30	0.15	180	8
K1	3.5	2.5	1.5	30	0.05	180	8
K2	3.5	2.5	1.5	30	0.10	180	8
K3	3.5	2.5	1.5	30	0.15	180	8
Note: the amount of Cr (VI) was calculated based on the Cr/Si molar ratio							

After CaO and quartz sand were mixed evenly, deionized water was added and stirred evenly with a magnetic stirrer. The mixture was then poured into a high-pressure reaction vessel lined with polytetrafluoroethylene and heated in a muffle furnace. The sample was heated and cooled to room temperature, then placed in a dryer to dry at 60 °C. The dried sample was ground, sieved through a 180 mesh sieve, and stored in a sealed bag.

2.3. Cr (VI) leaching experiment

The sample in section 2.2 was poured into deionized water (liquid-solid ratio of 10) and placed on a speed controlled horizontal oscillator for 8 hours of oscillation. After oscillation, it was left to stand for 16 hours and filtered using medium speed qualitative filter paper. The

filtrate was placed in a sample retention tube for testing. Filter residue and filter paper are stored in sealed bags.

2.4. Characterization methods

The phase composition and microstructure of C-S-H were characterized using X-ray diffraction (XRD), Fourier transform infrared (FTIR) spectrometer, and scanning electron microscope (SEM). XRD measurement conditions: copper target (40 kV and 40 mA), scanning angle of 5 – 70°, and scanning speed of 2°/min. FTIR (VERTEX 70) was used to determine the polymerization state of silicon-oxygen chains in C-S-H, with a test range of 4000 – 400 cm^{-1}. The microstructure was observed using a NOVA field emission SEM with an acceleration voltage of 10 kV.

The Cr(VI) content of the filtrate in section 2.3 was measured using atomic absorption spectrophotometry with an AA800 flame atomic absorption spectrophotometer (P-E, USA). Instrument working conditions: wavelength 357.9 nm; lamp current 7.0 mA; slit width 0.2 nm. Selected working conditions for graphite furnace: drying at 130 °C for 25 seconds; ashing at 1500 °C for 20 seconds; atomization at 2300 °C for 5 seconds.

3. RESULTS AND DISCUSSION

3.1. Phase compositions of C-S-H doped with Cr(VI)

3.1.1. Effects of Ca/Si ratio

The solidification of Cr(VI) by C-S-H under different Ca/Si ratios was first studied due to that the reaction products largely depend on the Ca/Si ratio in the CaO-SiO_2-H_2O system. Fig. 2 shows the XRD patterns of C-S-H with different Ca/Si ratios. It is demonstrated that the main hydration products are C-S-H (2θ = 29.3°) [16] and C-S-H (I) (2θ = 29.0 °) [23] when Ca/Si = 0.5, and their peak shapes are dispersed.

In addition, there are also calcium carbonate and unreacted quartz. After doping the Cr(VI), the intensity of characteristic peaks attributed to C-S-H and C-S-H (I) tends to be weaker, and the calcium dichromate phase (2θ = 24.6°, 33.5°) appears, indicating that Cr(VI) exists in the hydration products in form of $CaCrO_4$. At the same time, the hydration reaction is blocked because the number of Ca^{2+} forming C-S-H gel is reduced due to the combination of Ca^{2+} with Cr(VI). When Ca/Si = 1, the main products are tobermorite (2θ = 7.8°, 16.2°, 29.0°, 30.0°, 31.8°, 49.6°, 54.9°) and C-S-H (2θ = 29.3°). The characteristic peaks of the tobermorite are sharp, indicating its high crystallinity. The formation of tobermorite is mainly determined by its stoichiometry ($Ca_5Si_6O_{16}(OH)_2 \cdot 4H_2O$) [24]. When Cr(VI) is doped, the characteristic peaks of tobermorite disappear, while the characteristic peaks of quartz appear (2θ = 20.8°, 26.6°, 39.5°, 59.9°), indicating that the introduction of Cr(VI) will hinder the crystallization of C-S-H, that is, the formation of tobermorite. This may be due to the participation of Cr(VI) in the formation process of C-S-H [18]. Substituting or replacing calcium or silicon, due to the large difference between the spacing between Cr-O and polyhedral Ca-O, which is 0.1672 nm and 0.1822 nm, reduces the basic structural parameters and causes deformation of the C-S-H structure, resulting in the inability to form tobermorite normally. In addition, due to the emergence of a new phase $CaCrO_4$, the number of Ca^{2+} forming the C-S-H gel is reduced, thus the hydration reaction is blocked [17]. When Ca/Si = 1.5, the main product is C-S-H (2θ = 29.3°) with a small amount of tobermorite (2θ = 7.7°, 28.8°, 30.0°).

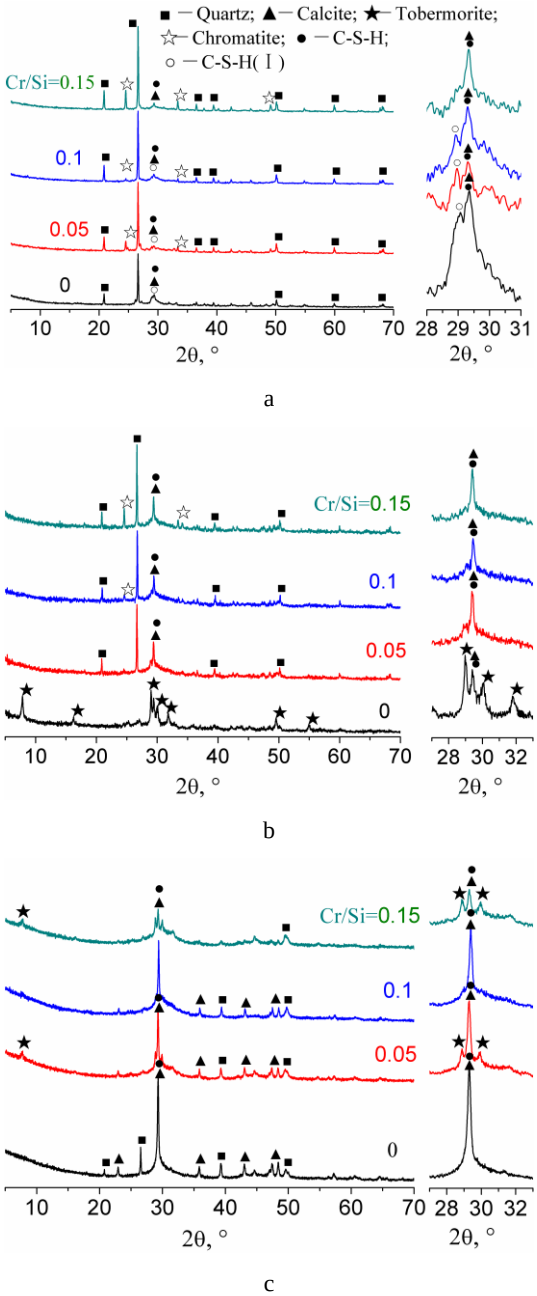

Fig. 2. XRD patterns of C-S-H with different Ca/Si ratios: a – Ca/Si = 0.5; b – Ca/Si = 1; c – Ca/Si=1.5

3.1.2. Effects of reaction temperature and time

The formation and crystallization process of C-S-H are also influenced by reaction temperature and time. Fig. 3 shows the XRD patterns of C-S-H (Cr/Si = 0.10) at different reaction temperatures. It can be seen from Fig. 3 that when the reaction temperature is 140 °C, the main products in the sample without Cr(VI) are C-S-H (2θ = 29.3°), calcium carbonate, and unreacted quartz.

When the reaction temperature is 180 °C, the products are tobermorite and a small amount of calcium carbonate. When the reaction temperature is 220 °C, the product mainly includes xonotlite. By comparison, tobermorite also appears at 220 °C in the case of Cr(VI). It can be concluded that increasing the reaction temperature is beneficial for the transformation of C-S-H into tobermorite and xonotlite, that is, to improve the crystallinity of C-S-H. After doping with Cr(VI), the crystallization of C-S-H is inhibited at 180 °C and 220 °C, which is consistent with the sample without Cr(VI). Besides, the characteristic peaks of the tobermorite phase disappear after Cr(VI) doping at 180 °C, and the hydration product is C-S-H (I). Also, Cr(VI) doping inhibits the formation of xonotlite at 220 °C, and the hydration products are xonotlite and tobermorite. The main reaction route of $CaO\text{-}SiO_2\text{-}H_2O$ is: C-S-H gel →C-S-H (I)→tobermorite→xonotlite, the crystallinity increases and gradually transforms into crystalline tobermorite and xonotlite as the temperature increases and reaction time prolongs [25 – 27]. It is displayed that Cr (VI) is more conducive to the stability of tobermorite at higher temperatures. It can be inferred that the formation process of C-S-H is affected by the changed structure influenced by Cr(VI). It is known that the growth of C-S-H crystals mainly occurs through the nucleation and growth of solid precursor C-S-H [28, 29].

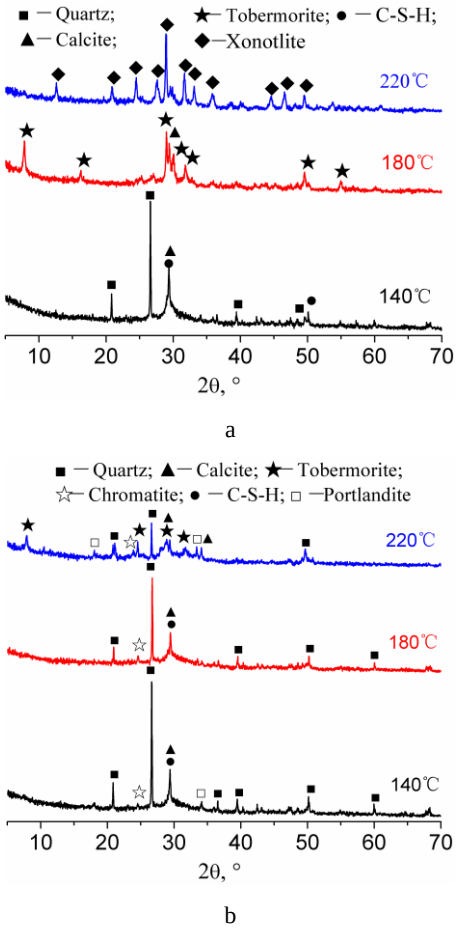

Fig. 3. XRD patterns of C-S-H at different reaction temperatures: a – Cr/Si=0; b – Cr/Si=0.10

The phase evolution with reaction time is presented in Fig. 4. As the reaction time prolongs, the diffraction peak intensity of the tobermorite increases, indicating a higher content of the tobermorite. After doping with Cr(VI), the diffraction peak intensity of C-S-H becomes weaker, while that of tobermorite becomes stronger, indicating that the crystallinity of C-S-H becomes higher. The crystallization of C-S-H is controlled by dissolution and precipitation, and with the increase in ion concentration, the continuous precipitation of calcium silicate nuclei leads to an increase in the crystallinity of C-S-H. Extending the reaction time is favorable for increasing the number of crystal nuclei and prolonging the crystal growth period. After doping with Cr(VI), the diffraction peaks of tobermorite disappear, and a new phase of $CaCrO_4$ is formed. With the increase of Cr(VI) doping, the peak intensity of $CaCrO_4$ increases, while the peak intensities of C-S-H (I) and C-S-H decrease, further indicating that Cr(VI) has an inhibitory effect on the crystallization of C-S-H.

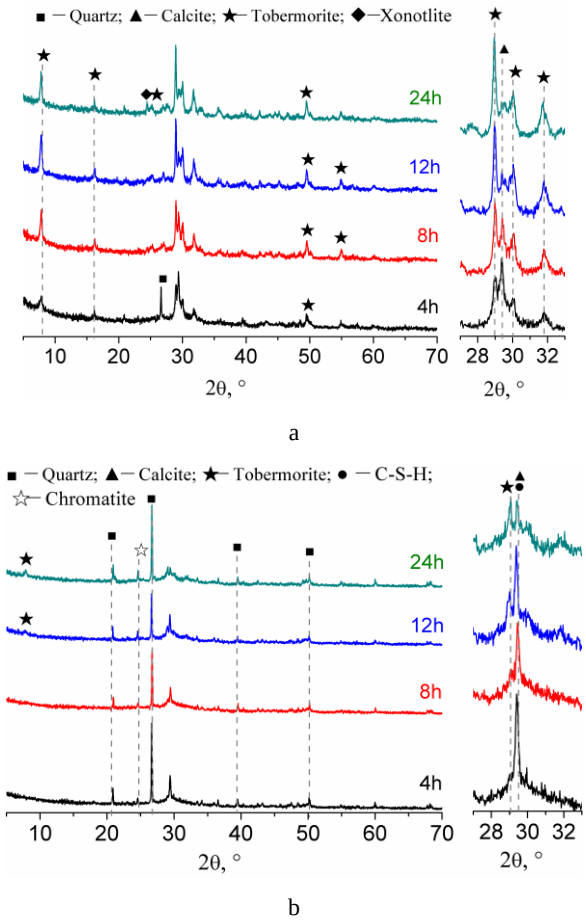

Fig. 4. XRD patterns of C-S-H at different reaction times: a – Cr/Si=0; b – Cr/Si=0.10

3.2. FTIR analyses

Fig. 5 displays the infrared spectra of C-S-H with different Cr/Si ratios. When Ca/Si is 0.5 and 1.0, the products contain Si-O-Si bonds (1084 cm^{-1}) and $[SiO_4]^{4-}$ group (970 cm^{-1}) [30, 31]. The difference is worth noting that the band around 970 cm^{-1} generated by Q^2 silicon sites is significantly stronger, especially when Ca/Si = 1.0. This phenomenon is closely related to the crystallization of tobermorite [30], which has a higher polymerization degree of silicate chains compared to C-S-H. Therefore, the FTIR results are consistent with the XRD analyses.

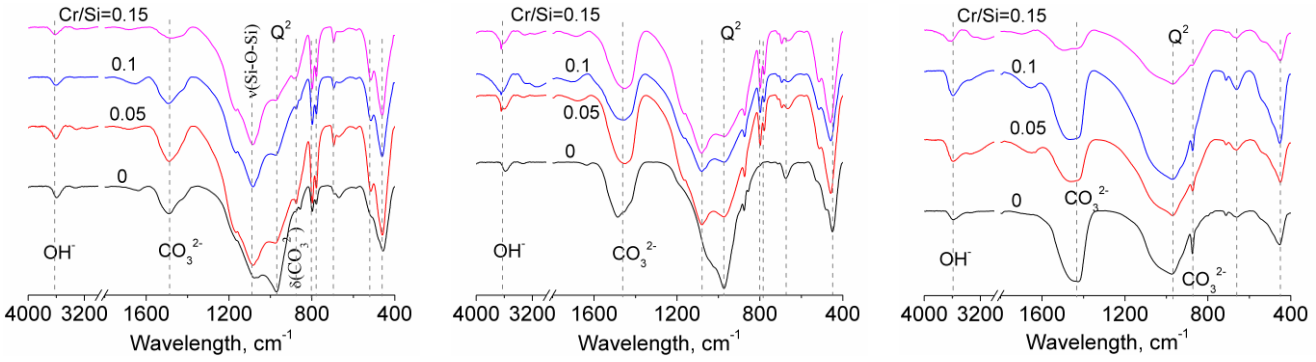

Fig. 5. Infrared spectra of C-S-H with different Cr/Si ratios: a – Ca/Si=0.5; b – Ca/Si=1; c – Ca/Si=1.5

As Cr/Si increases, the absorption peaks of $[SiO_4]^{4-}$ groups become flatter and the peak of Si-O-Si becomes sharper, indicating that the addition of Cr(VI) causes the bonds of $[SiO_4]^{4-}$ groups to break, shortening their chain length and affecting the formation of C-S-H. When Ca/Si is 1.5, there is no Si-O-Si bond in the product, and the absorption peak (873 cm^{-1}) intensity of CO_3^{2-} gradually weakens, while the vibration peak of the $[SiO_4]^{4-}$ group remains basically unchanged.

The infrared spectra shown in Fig. 6 and Fig. 7 help understand the effects of reaction temperature and time. It can be seen from Fig. 6. that as the reaction temperature increases, the peak of Si-O-Si becomes smoother, the peak of $[SiO_4]^{4-}$ group becomes sharper, and the width of the peak becomes narrower, indicating that the product develops towards a higher degree of polymerization.

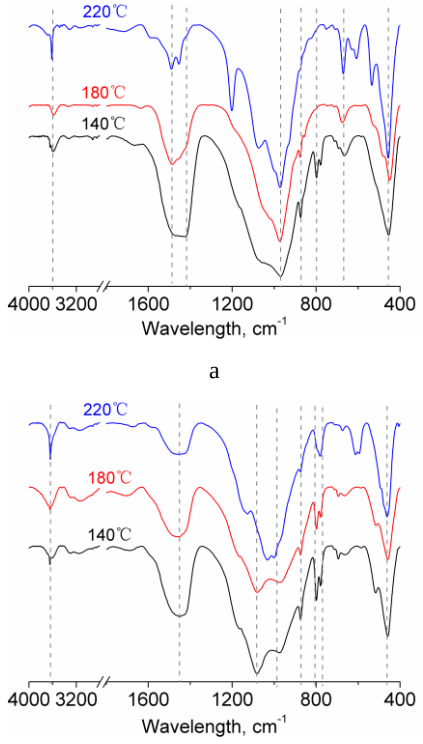

Fig. 6. Infrared spectra of C-S-H at different reaction temperatures: a – Ca/Si=0; b – Ca/Si=0.10

This is related to the increase in crystallinity of C-S-H, which can be confirmed by XRD analyses. In comparison, the introduction of Cr(VI) leads to weakening vibration peak intensity of $[SiO_4]^{4-}$, destroys the bonds in the $[SiO_4]^{4-}$, and affects the crystallization of C-S-H, which is consistent with the XRD analyses.

It is indicated in Fig. 7. that there is no Si-O-Si bond in the sample without Cr(VI), and the peak of the $[SiO_4]^{4-}$ group becomes sharper as the reaction time prolongs. After doping with Cr(VI), as the reaction temperature increases, and the reaction time prolongs, the Si-O-Si peak becomes smoother and the width of $[SiO_4]^{4-}$ group peak becomes narrower, indicating that the C-S-H product tends towards a higher degree of polymerization [32].

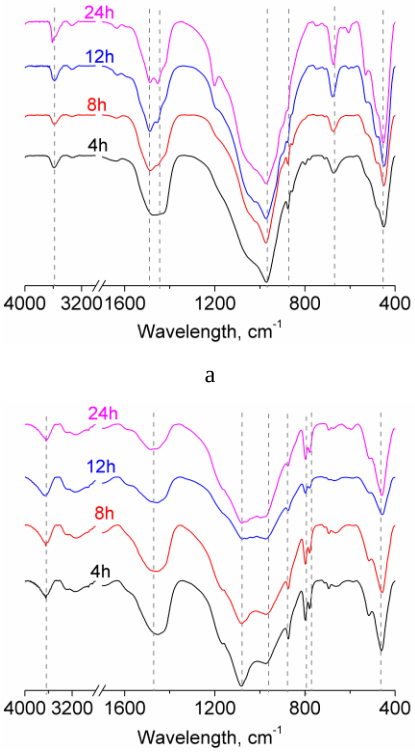

Fig. 7. Infrared spectra of C-S-H at different reaction times: a – Ca/Si=0; b – Ca/Si=0.10

3.3. Microscopic morphology and energy spectrum analyses

Fig. 8 shows the SEM images of the samples. The morphology of the sample without Cr(VI) is a coexistence of flocculent and flaky shapes, with high calcium and

silicon content. This is due to the presence of low crystallinity C-S-H and a small amount of tobermorite [27].

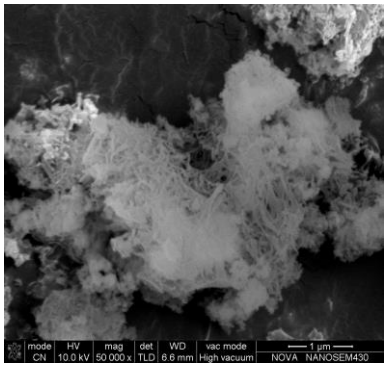

a

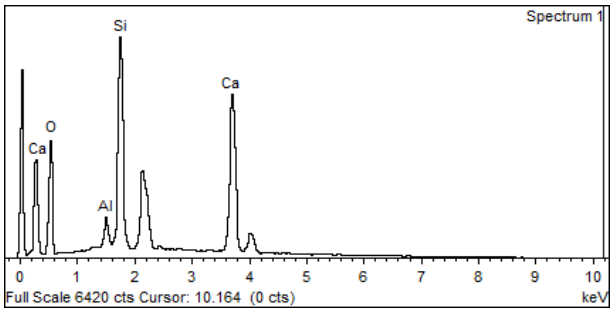

b

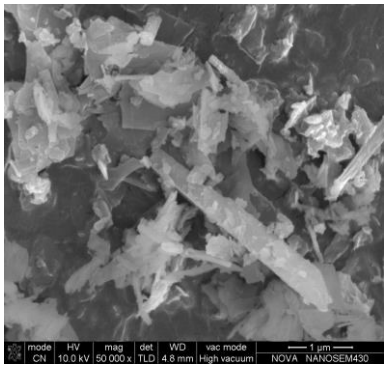

c

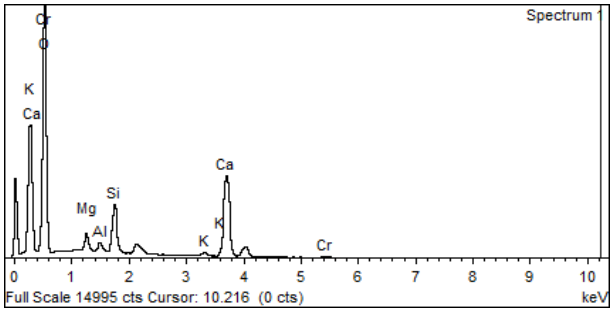

d

Fig. 8. SEM images: a – SEM image of C-S-H with Cr/Si=0; b – EDX result of C-S-H with Cr/Si=0; c – SEM image of C-S-H with Cr/Si=0.1; d – EDX result of C-S-H with Cr/Si=0.1

The morphology of sample doping Cr(VI) is sheet-like or plate-like, that is, the product is mainly composed of tobermorite, as confirmed in the energy dispersive X-ray spectroscopy (EDX) results. Other literature has also reported that sheet-like or plate-like is a typical microstructure of tobermorite [25, 30, 32, 35]. In addition, EDX results show that chromium element is present around tobermorite, which may be attributed to the formation of $CaCrO_4$ according to XRD analysis. It can be inferred that the addition of lower concentrations of Cr(VI) is beneficial for the formation of tobermorite, which increases the crystallinity of C-S-H.

3.4. Chromium leaching results and analyses

The dissolution amount of Cr(VI) is measured by atomic absorption spectrometer, and the solidification rate of Cr(VI) is calculated, the results are listed in Table 3.

From groups A, H, and K, it can be seen that under other constant conditions, the higher the Cr/Si ratio, the lower the solidification rate. This may be due to the higher concentration of Cr(VI) added, which inhibits the formation of C-S-H and provides less effective solidification ingredients. From B1, A2, C1, and D1, it can be seen that extending the reaction time appropriately (4 – 12 h) is beneficial for improving the solidification rate, but too long time (24 h) is detrimental to the solidification of Cr(VI). It can be seen in E1, A2, and F1 that an appropriate reaction temperature can achieve a better solidification rate, while a temperature that is too low or too high is not conducive to the solidification stability. This may be because the longer the reaction time and the higher the reaction temperature, the higher the crystallinity of C-S-H, and the appearance of the tobermorite phase in the product [34, 35]. However, tobermorite has weaker solidification stability for Cr(VI) than C-S-H. As demonstrated by Renata and Jan's research, the C-S-H gel synthesized at room temperature exhibits high solidification rates for Cd, Zn, Pb, and Cr cations, which can exceed 99.96 % [16]. Therefore, adjusting the crystallization process of C-S-H to control the ratio of crystalline and amorphous products is a challenge in optimizing the solidification of Cr (VI) under hydrothermal conditions.

Table 3. Solidification rate (SR) of Cr(VI) by C-S-H

No.	A1	A2	A3	B1	C1	D1	E1
SR, %	91.16	84.02	83.71	82.73	85.26	75.09	69.43
No.	F1	H1	H2	H3	K1	K2	K3
SR, %	73.06	71.04	61.99	56.48	74.21	71.45	62.09

4. DISCUSSION AND FUTURE WORK

The use of cement-based materials to solidify heavy metal ions and reduce environmental risks has been one of the research hotspots in the environmental field. The main product of cement-based materials, C-S-H, adsorbs and solidifies heavy metal ions mainly through physical encapsulation, chemical adsorption, and other methods, but there are certain differences in the solidification mechanism of different heavy metal ions. The structure of C-S-H is greatly affected by chemical compositions and environmental conditions. At room temperature, C-S-H is mainly amorphous, i.e., C-S-H gel. Because of its large specific surface area, this structure has strong adsorption for heavy metal ions.

As the application range of cement-based materials becomes wider, their hydration environmental conditions also vary greatly, such as steam curing or autoclaved curing, and deep geological conditions such as oil wells or geothermal fields. Under high-temperature and high-pressure environments, the crystallinity of C-S-H increases, and heavy metal ions will also affect the crystallization process and their solidifications. This work indicates that Cr (VI) does indeed affect the crystallization of C-S-H. The formation of the new compound $CaCrO_4$ changes the concentration of Ca^{2+} in the system to a certain extent, which may interrupt the ongoing crystallization process, i.e., the transition from tobermorite to xonotlite, thereby stabilizing C-S-H on the tobermorite structure and improving the stability of tobermorite.

There have been investigations on the porous structure of tobermorite and its adsorption effect on heavy metal ions [35, 36]. Therefore, cement-based materials still have a better solidification effect on Cr (VI) under hydrothermal conditions, which provides the foundation for expanding the application of cement-based materials in extreme environments. Of course, future work will focus on the solidification behavior of other heavy metal ions, such as Cd, Pb, Cu, Zn, Ni, etc., under hydrothermal conditions.

5. CONCLUSIONS

In order to clarify the solidification of Cr (VI) by C-S-H and expand the application of cement-based materials for solidifying heavy metal ions in high temperature and high pressure environments, C-S-H was synthesized by hydrothermal method and the solidification effect of Cr(VI) in C-S-H was studied in this work, the following major conclusions can be drawn:

1. The reaction temperature, holding time, and Cr(VI) content have an impact on the crystallinity of C-S-H. As the temperature is below 220 °C and the reaction time is within 24 hours, appropriately increasing the reaction temperature and prolonging the reaction time can help improve the crystallinity of C-S-H. A small dosage of $Cr/Si < 0.05$ is beneficial for the crystallization of C-S-H, but when $Cr/Si > 0.10$, Cr(VI) inhibits the crystallization of C-S-H.
2. The factors that affect the solidification stability of C-S-H on Cr(VI) include the Ca/Si ratio, Cr/Si ratio, reaction temperature, and holding time. The higher the Cr/Si (< 0.15) ratio, the lower the solidification rate of Cr(VI). A Ca/Si ratio of 1.0, appropriate reaction time (4 – 12 h), and reaction temperature (180 °C) can achieve a high solidification rate. The C-S-H with a Ca/Si ratio of 1.0, 180 °C, and 8 h has the highest solidification rate of Cr(VI).

Acknowledgments

This work is financially supported by the Guangdong Basic and Applied Basic Research Foundation (No. 2024A1515010876), Research Platforms and Projects for Higher Education Institutions of Guangdong Province (No. 2023ZDZX4056), National Natural Science Foundation of China (No. 52002245), Scientific Research Projects of Shaoguan University (No. SZ2021KJ01, 408/99000623), Science and Technology Plan Project of Shaoguan City (No. 210726194533404, No. 230313096271964, No. 240901198038599).

REFERENCES

1. **Niu, X., Elakneswaran, Y., Hiroyoshi, N.** Surface Chemistry and Radionuclide Anion Immobilisation Potential of Phosphoric Acid-Activated Metakaolin-Based Geopolymers *Cement and Concrete Research* 181 2024: pp. 107549. https://doi.org/10.1016/j.cemconres.2024.107549
2. **Fan, C., Wang, B., Xu, Y.** Solidification/Stabilization and Immobilization Mechanism of Pb(II) and Zn(II) in Ettringite *Cement and Concrete Research* 174 2023: pp. 107350. https://doi.org/10.1016/j.cemconres.2023.107350
3. **Bakhshi, N., Sarrafi, A., Ramezanianpour, A.A.** Immobilization of Hexavalent Chromium in Cement Mortar: Leaching Properties and Microstructures *Environmental Science and Pollution Research* 26 (20) 2019: pp. 20829 – 20838. https://doi.org/10.1007/s11356-019-05301-z
4. **Husnain, A., Qazi, I.A., Khaliq, W., Arshad, M.** Immobilization in Cement Mortar of Chromium Removed from Water Using Titania Nanoparticles *Journal of Environmental Management* 172 2016: pp. 10 – 17. https://doi.org/10.1016/j.jenvman.2016.02.026
5. **Wang, S., Vipulanadan, C.** Solidification/Stabilization of Cr(VI) with Cement – Leachability and XRD analyses *Cement and Concrete Research* 30 (3) 2000: pp. 385 – 389. https://doi.org/10.1016/S0008-8846(99)00265-3
6. **Peysson, S., Péra, J., Chabannet, M.** Immobilization of Heavy Metals by Calcium Sulfoaluminate Cement *Cement and Concrete Research* 35 (12) 2005: pp. 2261 – 2270. https://doi.org/10.1016/j.cemconres.2005.03.015
7. **Małolepszy, J., Deja, J.** Immobilization of Heavy Metals Ions by the Alkali Activated Slag Cementitious Materials *Studies in Environmental Science* 60 1994: pp. 519 – 524. https://doi.org/10.1016/S0166-1116(08)71484-5
8. **Valls, S., Vazquez, E.** Stabilisation and Solidification of Sewage Sludges with Portland Cement *Cement and Concrete Research* 30 2000: pp. 1671 – 1678. https://doi.org/10.1016/S0008-8846(00)00363-X
9. **Giergiczny, Z., Król, A.** Immobilization of Heavy Metals (Pb, Cu, Cr, Zn, Cd, Mn) in the Mineral Additions Containing Concrete Composites *Journal of Hazardous Materials* 160 2008: pp. 247 – 255. https://doi.org/10.1016/j.jhazmat.2008.03.007
10. **Wang, D., Ma, B., Pang, L., Wang, Q.** Alkali-Activated Blast Furnace Ferronickel Slag for Cr Immobilization *Cement and Concrete Composites* 150 2024: pp. 105560. https://doi.org/10.1016/j.cemconcomp.2024.105560
11. **Wang, J., Shi, D., Xia, Y., Liu, M., Ma, X., Yu, K., Zhao, Y., Zhang, J.** Stabilization/Solidification of Radioactive Borate Waste via Low-Carbon Limestone Calcined Clay Cement (LC3) *Journal of Environmental Chemical Engineering* 12 (3) 2024: pp. 113129. https://doi.org/10.1016/j.jece.2024.113129
12. **Xu, J.Z., Zhou, Y.L., Chang, Q., Qu, H.Q.** Study on the Factors of Affecting the Immobilization of Heavy Metals in Fly Ash-Based Geopolymers *Materials Letters* 60 2006: pp. 820 – 822. https://doi.org/10.1016/j.matlet.2005.10.019
13. **Luo, Z., Zhi, T., Liu, L., Mi, J., Zhang, M., Tian, C., Si, Z., Liu, X., Mu, Y.** Solidification/Stabilization of Chromium Slag in Red Mud-Based Geopolymer *Construction and Building Materials* 316 2022: pp. 125813. https://doi.org/10.1016/j.conbuildmat.2021.125813

14. **Pointeau, I., Marmier, N., Fromage, F., Fedoroff, M., Giffaut, E.** Cesium and Lead Uptake by CSH Phases of Hydrated Cement *MRS Online Proceedings Library* 663 2000: pp. 97. https://doi.org/10.1557/PROC-663-97a
15. **Niuniavaite, D., Baltakys, K., Dambrauskas, T., Eisinas, A.** Cu^{2+}, Co^{2+} and Cr^{3+} Adsorption by Synthetic Dibasic Calcium Silicate Hydrates and Their Thermal Stability in A 25-1000 °C Temperature Range *Journal of Thermal Analysis and Calorimetry* 138 2019: pp. 2241 – 2249. https://doi.org/10.1007/s10973-019-08795-4
16. **Renata, Z., Jan, D.** Spectroscopy Study of Zn, Cd, Pb and Cr Ions Immobilization on C-S-H Phase *Spectrochimica Acta Part A Molecular & Biomolecular Spectroscopy* 134 2015: pp. 614 – 620. https://doi.org/10.1016/j.saa.2014.06.069
17. **Zheng, X., Zhang, N., Nan, J., Hou, X., Tan, H., Guo, C.** The Solidification Mechanism of Portland Cement for Cr Ions and its Application in the Solidification of Iron Slag *Nonferrous Metal Materials and Engineering* 37 (2) 2016: pp. 34 – 40. (in Chinese) https://link.cnki.net/doi/10.13258/j.cnki.nmme.2016.02.006
18. **Guo, X., Ma, H., Zhou, J., Cheng, W., Ba, M.** Stabilization Mechanism of Hexavalent Chromium Ions in Portland Cement-Based Materials *Case Studies in Construction Materials* 20 2024: pp. e03110. https://doi.org/10.1016/j.cscm.2024.e03110
19. **Lü, Y., Geert, D.** Polymorph Transformation of Tricalcium Silicate Doped with Heavy Metal *Journal of Wuhan University of Technology-Materials Science* 31 (4) 2016: pp. 883 – 890. https://doi.org/10.1007/s11595-016-1463-z
20. **Omotoso, O., Ivey, D.** Hexavalent Chromium in Tricalcium Silicate: Part II Effects of Cr(VI) on the Hydration of Tricalcium Silicate *Journal of Materials Science* 33 (2) 1998: pp. 515 – 522. https://doi.org/10.1023/A:1004356805022
21. **Yao, Y., Wang, X., Yan, B., Wang, L., Liu, C.** The Research on Heavy Metal Ions Curing and Its Influence on the Cement Hydration Process *Bulletin of the Chinese Ceramic Society* 31 (5) 2012: pp. 1138 – 1144. (in Chinese) https://link.cnki.net/doi/10.16552/j.cnki.issn1001-1625.2012.05.033
22. **Zhao, S., Chen, Z., Zhang, T., Peng, X., Zhang, Y., Ding, Z., Lei, J.** Advances in Solidification/Stabilization Technology Treatment of Heavy Metals in Contaminated Soils *Chinese Journal of Soil Science* 44 (6) 2013: pp. 1531 – 1536. (in Chinese) https://link.cnki.net/doi/10.19336/j.cnki.trtb.2013.06.044
23. **Baltakys, K., Eisinas, A., Baltakys, M., Siauciunas, R.** Incorporation of Insoluble Heavy Metal Oxide in Structure of Z Phase during Hydrothermal Treatment *Advances in Applied Ceramics* 113 (8) 2014: pp. 466 – 471. http://dx.doi.org/10.1179/1743676114Y.0000000145
24. **Hong, S.Y., Glasser, F.P.** Phase Relations in the CaO–SiO_2–H_2O System to 200 °C at Saturated Steam Pressure *Cement and Concrete Research* 34 2004: pp. 1529 – 1534. https://doi.org/10.1016/j.cemconres.2003.08.009
25. **Shaw, S., Clark, S.M., Henderson, C.M.B.** Hydrothermal Formation of the Calcium Silicate Hydrates, Tobermorite ($Ca_5Si_6O_{16}(OH)_2$•$4H_2O$) and Xonotlite ($Ca_6Si_6O_{17}(OH)_2$): An In Situ Synchrotron Study *Chemical Geology* 167 (1 – 2) 2000: pp. 129-140. https://doi.org/10.1016/S0009-2541(99)00205-3
26. **Richardson, I.R.** Tobermorite/Jennite- and Tobermorite/Calcium Hydroxide-Based Models for the Structure of C–S–H: Applicability to Hardened Pastes of Tricalcium Silicate, *β*-Dicalcium Silicate, Portland Cement, and Blends of Portland Cement with Blast-Furnace Slag, Metakaolin or Silica Fume *Cement and Concrete Research* 34 2004: pp. 1733 – 1777. https://doi.org/10.1016/j.cemconres.2004.05.034
27. **Nocuń-Wczelik, W.** Effect of Na and Al on the Phase Composition and Morphology of Autoclaved Calcium Silicates Hydrates *Cement and Concrete Research* 29 1999: pp. 1759 – 1767. https://doi.org/10.1016/S0008-8846(99)00166-0
28. **Gougar, M.L.D., Scheetz, B.E., Roy, D.M.** Ettringite and C–S–H Portland Cement Phases for Waste Ion Immobilization: A Review *Waste Management* 16 (4) 1996: pp. 259 – 303. https://doi.org/10.1016/S0956-053X(96)00072-4
29. **Deja, J.** Immobilization of Cr(VI), Cd(II), Zn(II) and Pb(II) in Alkali-Activated Slag Binders *Cement and Concrete Research* 32 2002: pp. 1971 – 1979. https://doi.org/10.1016/S0008-8846(02)00904-3
30. **Mostafa, N.Y., Shaltout, A.A., Omar, H., Abo-El-Enein, S.A.** Hydrothermal Synthesis and Characterization of Aluminium and Sulfate Substituted 1.1 nm Tobermorites *Journal of Alloys and Compounds* 467 (1 – 2) 2009: pp. 332 – 337. https://doi.org/10.1016/j.jallcom.2007.11.130
31. **Yu, P., Kirkpatrick, R.J., Poe, B., McMillan, P.F., Cong, X.** Structure of Calcium Silicate Hydrate (C–S–H): Near-, Mid-, and Far-Infrared Spectroscopy *Journal of the American Ceramic Society* 82 (3) 1999: pp. 742 – 748. https://doi.org/10.1111/j.1151-2916.1999.tb01826.x
32. **Garcia-Lodeiro, I., Fernandez-Jimenez, A., Blanco-Varela, M.Z., Palomo, A.** FTIR Study of the Sol–Gel Synthesis of Cementitious Gels: C–S–H and N–A–S–H *Journal of Sol-Gel Science and Technology* 45 2008: pp. 63 – 72. https://doi.org/10.1007/s10971-007-1643-6
33. **Luo, F., Wei, C., Xue, B., Wang, S., Jiang, Y.** Dynamic Hydrothermal Synthesis of Al-Substituted 11 Å Tobermorite from Solid Waste Fly Ash Residue-Extracted Al_2O_3 *Research on Chemical Intermediates* 39 2013: pp. 693 – 705. https://doi.org/10.1007/s11164-012-0590-1
34. **Astrup, T., Mosbć, H., Christensen, T.H.** Assessment of Long-Term Leaching from Waste Incineration Air-Pollution-Control Residues *Waste Management* 26 2006: pp. 803 –-814. https://doi.org/10.1016/j.wasman.2005.12.008
35. **Zhao, Z., Wei, J., Li, F., Qu, X., Shi, L., Zhang, H., Yu, Q.** Synthesis, Characterization and Hexavalent Chromium Adsorption Characteristics of Aluminum- and Sucrose-Incorporated Tobermorite *Materials* 10 (6) 2017: pp. 597. https://doi.org/10.3390/ma10060597
36. **Tsutsumi, T., Nishimoto, S., Kameshima, Y., Miyake, M.** Hydrothermal Preparation of tobermorite from Blast Furnace Slag for Cs^+ and Sr^{2+} Sorption *Journal of Hazardous Materials* 266 2014: pp. 174 – 181. https://doi.org/10.1016/j.jhazmat.2013.12.024